Application of MEMS Technologies to Nanodevices

Lance Doherty,[‡] Hongbing Liu, Veljko Milanović

Adriatic Research Institute
2131 University Ave., Suite 322
Berkeley, CA 94704
{hliu,veljko}@adriaticresearch.org

[‡]Berkeley Sensor and Actuator Center
497 Cory Hall #1770
University of California at Berkeley, Berkeley, CA 94720
ldoherty@eecs.berkeley.edu

***Abstract* – A process methodology enabling the fabrication of various nanodevices is demonstrated that is compatible with standard integrated circuit processes and recently developed MEMS technologies. The basic devices are laterally suspended single-crystal silicon nanowires with diameters from ~20 nm formed by a single DRIE etch step and oxidation thinning cycles. These nanowires can further serve as molds for conformal polysilicon and silicon nitride deposition, resulting in coaxial nanowires and fluidic devices such as nanocapillaries and nanopores with <100 nm inner diameters. The above nanodevices are being investigated for use in thermoelectric and biomedical applications as well as MEMS actuator integration.**

I. Introduction

Nanowires and other low-dimensional structures have been widely used to study material property changes as size scales decrease. These nanowires have also been explored for various applications (e.g. [1]-[5]). Silicon nanowires (SiNWs) exhibit a direct band gap and have been demonstrated for luminescent applications [1]. Quantum confinement effects in nanowires allow the development of single electron devices [2], and the Coulomb blockade has been observed [3]. Field emission from single-ended nanowires is aided by electric field magnifications due to small tip radii [4]. Biological and chemical specimens are controllable and detectable with nanowires of the same scale [5]. However, controlled mass production, and especially integration of nanowires into potential applications remains a challenge.

SiNWs in particular are compatible with well-established integrated-circuit (IC) processes, for example, modifying material properties through doping. There are two major reported thrusts in SiNW fabrication research. The first grows the wires with a metal catalyst in either a vapor-liquid-solid [6] or a solution-phase [7] process. These wires are difficult to contact individually as they grow vertically. Potential contamination of integrated circuits by the catalyst metals and difficulty of obtaining ohmic electrical contacts at either end are other disadvantages. The alternative thrust uses e-beam lithography to directly trace a lateral SiNW in a thin silicon surface and etches all but the thin nanowire atop an insulator [8]. This method requires costly and time-consuming lithography and is typically done in a device layer of polysilicon with its inherent grain boundaries that may adversely affect device performance.

We previously demonstrated the mass fabrication of lateral single-crystal SiNWs with a simple process [9]. Our methodology utilizes widely available and low-cost optical lithography, basic deposition and thermal oxidation furnaces and the inductively coupled plasma etcher often used to fabricate MEMS devices. The simple and low-cost methodology provides isolated and suspended lateral SiNWs as well as dense arrays of lateral SiNWs that are directly contacted to probing pads, can be selectively doped, have arbitrary mask-defined topologies, and can be thinned to desired cross-sectional diameters.

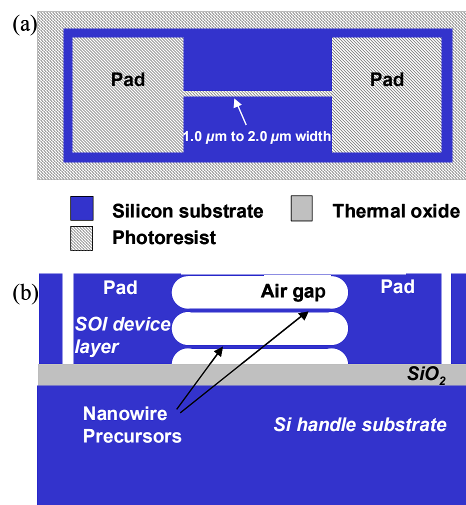

Figure 1. Fabrication of SiNWs by DRIE etching of SOI wafers: (a) Schematic of layout of a nanowire, probing pads and isolating trenches, (b) Schematic cross-section of the structures following three pulses of DRIE.

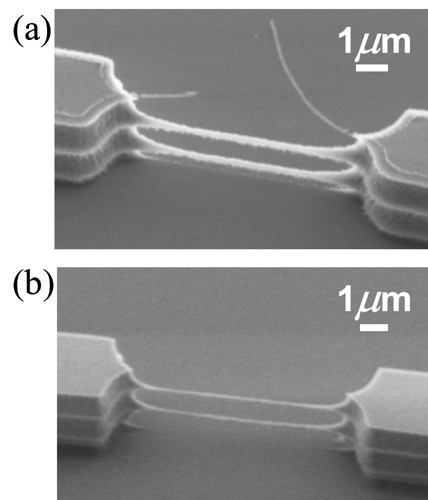

Figure 2. A single device at different stages of fabrication: (a) Following three pulses of DRIE, (b) Following two oxidation thinning cycles, the wire has a diameter of 70nm.

II. Fabrication

A. Etching and Oxidation-Thinning of Nanowires

Our low-cost SiNWs are lithographically defined with a single mask and created with a single etch step in a standard 1 μm microfabrication technology. A simple device layout is depicted in Figure 1a. Narrow lines of photoresist (from 1 μm to 2 μm) for SiNWs and larger blocks for probing pads are patterned. Initial minimum SiNW diameters are bounded by

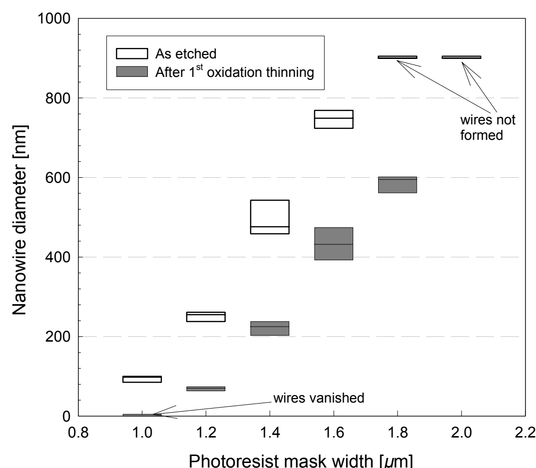

Figure 3. Different nanowire diameters result from changing the photoresist width in layout. White boxes show diameters prior to oxidation thinning while shaded boxes show diameters following a single oxidation cycle.

photoresist linewidth. The integration of our nanowire process with MEMS is directly possible if SOI wafers are used in the process, a substitution otherwise transparent to the fabrication.

Our method of etching the silicon nanowires is based on the cyclical nature of the deep reactive ion etch (DRIE) [10]. As a consequence of repeated isotropic etching and passivating steps, DRIE trench sidewalls are not smooth, but scalloped. This commonly undesired scalloping effect of DRIE can be utilized to fabricate sharp field emission tips and arrays [11]. The same phenomenon lends itself to the fabrication of nanowire precursors (Figure 1a) as the vertical scalloping effect (Figure 1b) etches right through the structure to create airgaps. After the DRIE, a set of vertically stacked wire precursors remains as defined lithographically with cross-sectional diameters ranging from ~50 nm to 100's of nm. These precursor wires are vertically stacked in quantity determined by the number of etch pulses. Modification of the DRIE parameters changes both the horizontal and vertical depths of the scalloping. Further shaping of the nanowire precursors into cylindrical cross-sections and diameter reduction is achieved by one or more thermal oxidation thinning cycles as detailed in [9] and shown in Figure 2 and Figure 3. Our process allows for repeating the nanowire stacks to exceed 10^8 nanowires per square centimeter of wafer area.

B. Coaxial nanowires

The basic methodology described above was augmented with a conformal polysilicon deposition to produce coaxial nanostructures. The polysilicon is deposited over the thin insulating oxide on the nanowires to allow independent conduction through the inner silicon and outer polysilicon layers. The outer layer is amenable to modifying the electrical and thermal properties of the inner nanowire. The thickness of the inner silicon is defined by the repetition of the thinning cycles while the thickness of insulating and outer layers are defined by the deposition times. The process flow is detailed in [9]. Devices fabricated by selectively patterning the polysilicon axial process are shown in Figure 4.

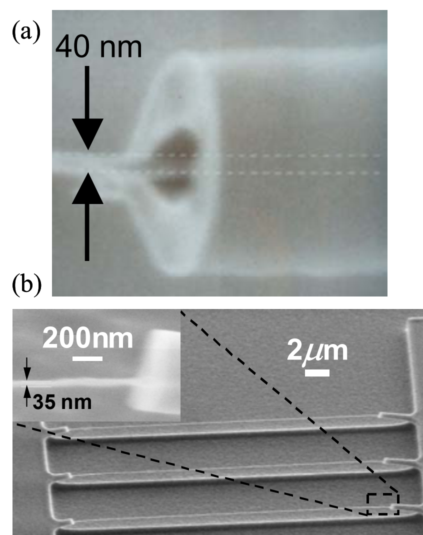

Figure 4. SEM of fabricated devices with polysilicon shielding of the silicon nanowires and oxide removed: (a) A coaxial wire with an inner diameter of 40 nm, (b) An array of coaxial wires showing the inner wires spanning a 20 μm gap.

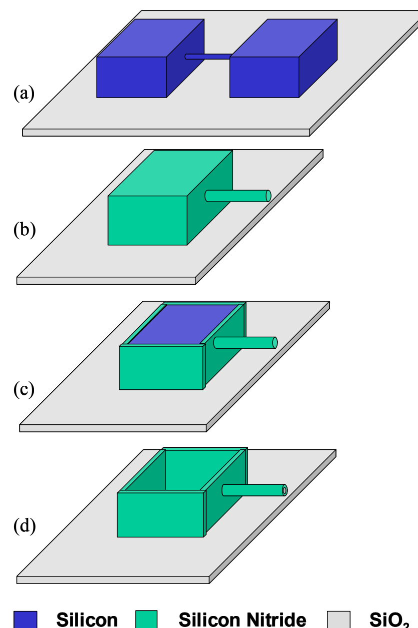

Figure 5. Fabrication of nanofluidic devices: (a) Original SiNW structure, (b) Conformal deposition of silicon nitride, (c) Removal of top layer of nitride, (d) XeF_2 removal of silicon mold.

C. Nanocapillaries and Nanopores

There has been increased interest recently in the possibility of utilizing nanometer-scale fluidic channels for a variety of bio-applications, and energy storage applications. It has been demonstrated (Han and Craighead [12], for example) that nanometer size gaps have promising bio-applications such as DNA separation. In their work however, nanowire-based (one-dimensional flow) nanocapillaries have not been demonstrated, and the technologies are difficult to integrate with present microfluidics and bioMEMS. We have been pursuing the following direction to overcome those limitations.

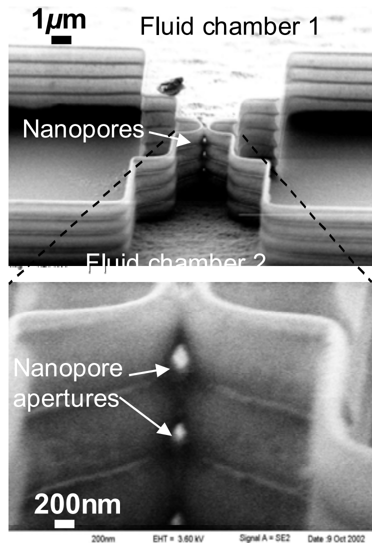

Figure 6. SEM of a fabricated nanofluidic device: (a) Nanopores join the two fluid chambers, (b) A detail of the junction illustrates the size of the nanopores.

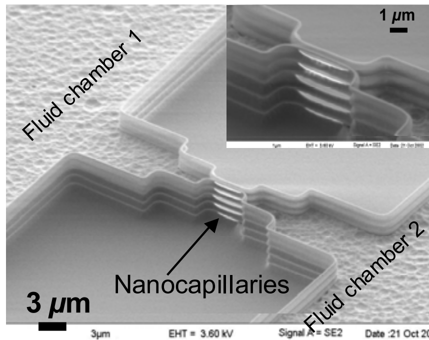

Figure 7. SEM of a fabricated nanocapillary device. Capillaries are 5μm long and all but the topmost are fully sealed (inset).

Figure 5 schematically shows the process for creating nanofluidic channels, or nanocapillaries, out of the previously shown SiNWs, now used as sacrificial molds. Figure 5a is the basic SiNW structure with the nanowire suspended between 2 pads. The wafer then undergoes 250 nm LPCVD silicon nitride deposition at 830 °C. The nitride deposits conformally all around the pads and the nanowires. Figure 5b shows this step schematically, though only half of the structure is now shown for clarity. Then in a chemical mechanical polishing (CMP) step, the top nitride coating is removed such that the single-crystal silicon is exposed on the pads (Figure 5c) allowing an isotropic silicon etch to completely remove the silicon pads and hollow out the nanowires. All silicon is etched away leaving the nitride wall to form nanocapillaries where the inner diameter reflects the diameter of the nanowire mold. Examples of fabricated structures are shown in Figure 6 and Figure 7. As can be seen in the fabricated devices, the nitride walls also form fluidic chambers at either end of the nanocapillary, making these devices suitable for experimentation.

Experiments with the fabricated nanocapillaries are currently on-going. Mirroring the variation in SiNW diameters from 10s of nanometers to 100s of nanometers, the fabricated fluidics channels have a variety of inner diameters. In the future, we hope to quantify and compare their functionality for passing fluids, ions and biomolecules as a function of diameter. The initial difficulty of selectively filling the small fluid chambers formed by the nitride walls has been overcome by the use of MicroFab's MicroJet technology. We controllably apply many small droplets of a saline solution into the chambers, filling chamber one (Figures 6 and 7) first. Example microphotographs of such filling experiments are shown in Figure 8. We then observed whether the solution passed through the nanocapillaries into chamber two. We noted that for larger diameters the solution passed through the channels, filling the second chamber due to the highly hydrophilic surfaces on the bottom and the sidewalls. However, for channels of estimated diameter below 100 nm, no leaking into the second chamber was observed, which we then filled separately. Experiments with ion flow through the nanocapillaries are inconclusive to date.

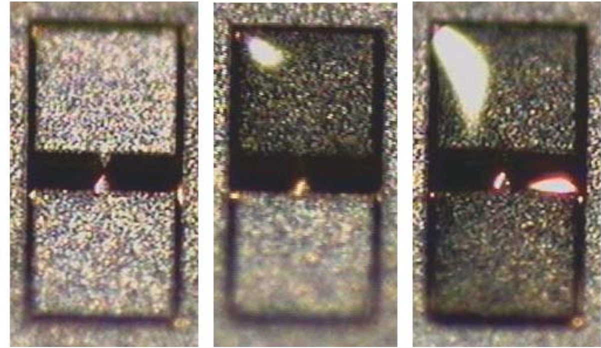

Figure 8. Micrographs of fluidic chambers and the connecting nanofluidic channels. Left: the structure before any solution filling. Middle: the top chamber is filled and no liquid passes into the bottom chamber. Right: filling of the top chamber eventually fills both chambers with liquid passing by the channel between them.

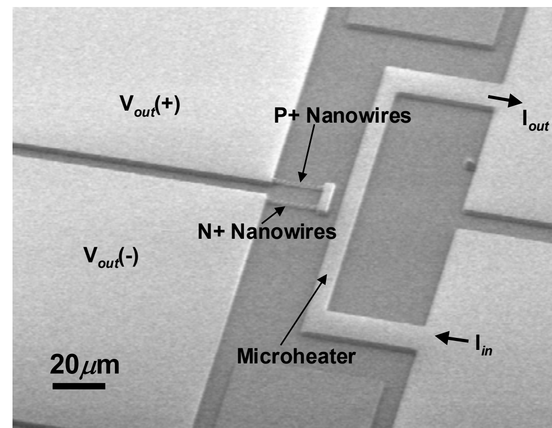

Figure 9. A thermocouple device using SiNWs with different doping as the asymmetry to induce voltage.

III. Application Areas

A. Thermoelectric

It has been shown that quantum confinement in one-dimensional structures such as nanowires may greatly enhance efficiency and overall performance in thermoelectric devices.

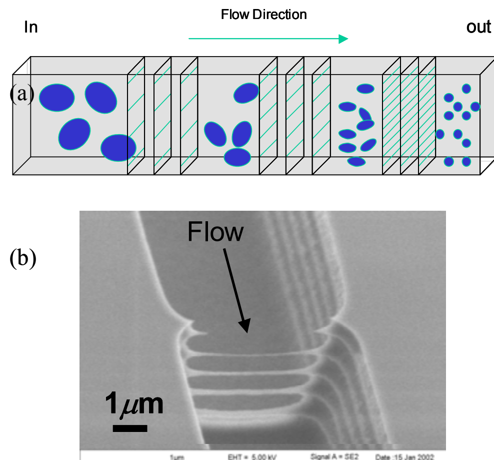

Figure 10. Biospecimen sorting and filtering can be accomplished by varying vertical wire separation along a channel: (a) Specimens of different sizes are stopped at different locations along a channel, (b) SEM of a single filter of the proposed device.

For that reason, many groups have been pursuing technologies to achieve such nanometer-based devices such as [13]. Our effort focuses on comparing basic thermocouple structures with bulk silicon arms with those made with thermocouples, to verify the theoretical expectations. In Figure 9, one such thermocouple device is shown. Asymmetry in the Seebeck coefficients of the two legs is introduced by doping the silicon with n and p impurities prior to the etch step. Such devices are currently being tested and evaluated. Initial results show that nanowire thermocouples have more drastic thermal behavior than their bulk counterparts, and a different effective Seebeck coefficient.

B. Biomedical

Stacked fixed-end wires in glass-sealed microfluidic channels can be utilized to filter and trap micrometer-sized bioorganisms such as cells. As schematically shown in Figure 10 the nanowires can be laid out along micro fluidic channels and stacked with decreasing sequential vertical wire spacing down the channel. When biological samples run through fluidic channels, they will be sorted and trapped based on their sizes for further study. Once filters have been clogged with specimens, either flow direction would have to be reversed to clean the channel of debris or the device would have to be discarded. Such filters can be used in combination with or replace current electrophoretic channels or chromatography columns. If such wire traps and filters are isolated electrically from other sets and have independently applied potential, electrophoretic flow can hence be applied and regulated at small distances within the channel with small voltages. The combination of mechanical/fluidic trapping and electrodes results in a type of gel-electrophoresis like device but with very low voltages, wide range of parameter control, and miniature package size.

Furthermore, the devices lend themselves as probes for biological specimens. Cell membranes become permeable to ions in the intra- and extra-cellular solutions when external voltages are applied to the membrane, a process known as electroporation. We have fabricated silicon nanowires with single ends anchored in a pad, while the other ends with atomically sharp tips protrude into the microchannel. Such electrode pairs can be integrated with microfluidic channels to trap and study living cells *in situ*. This technology can be integrated with MEMS positioning devices in the same DRIE process to actuate the probes towards and into the specimen. Such electrostatic comb-drive devices have been demonstrated with sharp tips [11], but not yet demonstrated in the presence of a buffer solution in which case isolation issues are yet to be resolved. One possibility is to attach the tips to thermal actuators instead which have also been demonstrated in air.

IV. Conclusions

We have successfully fabricated single-crystal silicon nanowires of various lengths and diameters in a simple etching process with oxidation-thinning. The process is a very low-cost way of achieving dense nanowire arrays that are easily electrically and thermally probed, easily integrated with gating electrodes, standard circuits, and MEMS. Their application in biodetection arrays, proteomics, nanoelectronics, or perhaps thermoelectrics may be possible with additional effort in process optimization, improved imaging capability to better determine final diameters and shapes of < 50 nm nanowires, and accurate doping control.

[1] D. P. Yu, *et al*, “Amorphous silica nanowires: Intensive blue light emitters,” Applied Physics Letters, **73**, no. 21, pp. 3076-3078, November 23, 1998.

[2] N. J. Stone, H. Ahmed, “Single-electron detector and counter,” Applied Physics Letters, **77**, no. 5, pp. 744-746, July 31, 2000.

[3] S.-W. Chung, *et al*, “Silicon nanowire devices,” Applied Physics Letters, **76**, no. 15, pp. 2068-2070, April 10, 2000.

[4] Y. H. Tang, *et al*, “Microstructure and field-emission characteristics of boron-doped Si nanoparticle chains,” Applied Physics Lett., **79**, no. 11, pp. 1673-1675, Sep. 10, 2001.

[5] Y. Cui, O. Wei, H. Park, C. M. Lieber, “Nanowire Nanosensors for Highly Sensitive and Selective Detection of Biological and Chemical Species,” Science, **293**, pp. 1298-1292.

[6] A. M. Morales and C. M. Lieber, “A laser ablation method for the synthesis of crystalline semiconductor nanowires,” Science, **279**, pp. 208-211, January 9, 1998.

[7] J. D. Holmes, K. P. Johnston, R. C. Doty, B. A. Korgel, “Control of thickness and orientation of solution-grown silicon nanowires,” Science, **287**, pp. 1471-1473, Feb. 25, 2000.

[8] A. C. Irvine, Z. A. K. Durrani, H. Ahmed, “Single-electron effects in heavily doped polycrystalline silicon nanowires,” Applied Physics Lett., **73**, no. 8, pp. 1113-1115, Aug. 24, 1998.

[9] V. Milanović, L. Doherty, “A simple process for lateral single-crystal silicon nanowires,” Proc. Of IMECE’02, New Orleans, LA, Nov 17-22, 2002.

[10] A. A. Ayon, *et al*, “Characterization of a time multiplexed inductively coupled plasma etcher,” Journal of the Electrochemical Society, **146**, no. 1, pp. 339-49, Jan. 1999.

[11] V. Milanović, *et al*, “Micromachining Technology for Lateral Field Emission Devices,” IEEE Tran. On Electron Devices, **48**, no. 1, pp. 166-173, Jan. 2001.

[12] J. Han, H. G. Craighead, “Separation of long DNA molecules in a microfabricated entropic trap array,” Science, **288**, pp. 1026-1029, May 12, 2000.

[13] A . Abramson, *et al*, “Nanowire Composite Thermoelectric Devices,” Proc. Of IMECE’02, New Orleans, LA, Nov. 17-22, 2002.